Phys. Scr. T129 (2007) 209–212 doi:10.1088/0031-8949/2007/T129/047

Deposition and sensing properties of PT/PZT/PT thin films for microforce sensors

Yan Cui[1], Hanbai Meng[3], Jing Wang[2], Weijie Dong[2] and Liding Wang[3]

[1] Key Laboratory for Precision and Non-traditional Machining Technology of Ministry of Education, 116023, China
[2] School of Electronic and Information Engineering, Dalian University of Technology, 116023, China
[3] Key Laboratory for Micro/Nano Technology and System of Liaoning Province, 116023, China

E-mail: yanc@dlut.edu.cn

Received 1 March 2007
Accepted for publication 6 September 2007
Published 28 November 2007
Online at stacks.iop.org/PhysScr/T129/209

Abstract

Microforce sensors made of PT/PZT/PT thin films were designed in the micro-Newton range. The PT/PZT/PT thin films were deposited on the Pt/Ti/SiO_2/Si substrate by the sol–gel process. Structure and the crystallinity of the deposited films were characterized. The sensing properties of the microforce sensors were measured in static state and in quasi-static state. The sensitivities of the microforce sensors with two different sizes were 0.004 and 0.040 $mV\mu N^{-1}$ in the quasi-static state.

PACS numbers: 77.65.Bn, 77.65.Ly, 81.70.Bt

(Some figures in this article are in colour only in the electronic version.)

www.spm.com.cn

1. Introduction

Pb(Zr, Ti)O_3 (PZT) thin films have been extensively studied due to their interesting ferroelectric, piezoelectric and pyroelectric properties. The structure of the thin films and in particular their preferred orientation will affect the materials properties and/or operation of the thin film devices [1]. Piezoelectric thin film materials and silicon technology have been used in ultrasonic micromotors [2], force sensors for scanning force microscopy [3], accelerometers [4, 5] and cantilever actuators [6, 7].

To obtain PZT thin films, a variety of thin film techniques including sputtering, laser deposition, sol–gel and metal-organic-chemical vapor deposition (MOCVD) have been developed. The sol–gel method is well suited for the preparation of thin layer ceramics because it offers several advantages, such as simplicity of the process, low cost and easy composition control [8]. However, phase development of PZT thin films is difficult due to the volatile PbO component which results in the low dielectric pyrochlore phase under lead deficient conditions. To overcome the above mentioned factors, a buffer layer between bottom electrode and PZT film is introduced to enhance the phase formation. Some reports on the buffer layer effects have been reported. Kwok and Desu [9] proposed an improved sol–gel process, by adding the PT buffer layer between the PZT thin films and substrate, which could offer nucleation sites to reduce the activation energy for the crystallization of PZT thin films. The crystallographic orientation is a key factor to affect the electric properties of the PZT thin films which affect the sensing property of the PZT microforce sensors. Ren *et al* [10] proposed a lead titanate (PT)/PZT/PT sandwich structure which has good dielectric and ferroelectric properties. Hidekazu *et al* [11] reported that a PT buffer layer of 20–40 Å thickness enhances the ferroelectric properties and homogeneous microstructure.

In this paper, we fabricated microforce sensors using PT/PZT/PT thin films and MEMS technology. The driving system and the testing system have been set up. The sensing properties of the microforce sensors have been measured in both static state and quasi static state.

2. Experimental

2.1. Deposition of PT/PZT/PT thin films

Precursor solutions for the PT and PZT thin films were prepared from lead acetate trihydrate [$Pb(CH_3COO)_2 \cdot 3H_2O$], zirconium nitrate pentahydrate [$Zr(NO_3)_4 \cdot 5H_2O$],

0031-8949/07/129209+04$30.00 © 2007 The Royal Swedish Academy of Sciences Printed in the UK

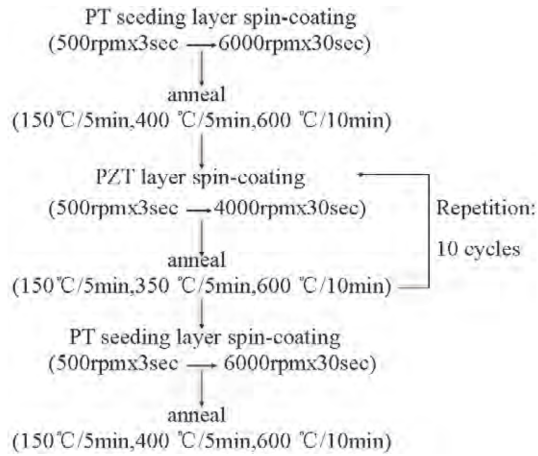

Figure 1. Flow diagram of the sol–gel process for the PT/PZT/PT thin film deposition.

titanium tetrabutoxide [$Ti(O(CH_2)_3CH_3)_4$], 2-methoxyethanol [$HOCH_2CH_2OCH_3$] and acetylacetone [$CH_3COCH_2COCH_3$] were used as the solvent and the chemical modifier. The Zr/Ti ratio was 53/47, 10% excess of lead was added to the precursor solutions to compensate for the loss of lead during the final annealing process. Figure 1 shows the flow diagram of the PT/PZT/PT thin films deposition technique based on the sol–gel process.

A PT buffer layer with thickness of 20 nm was coated and pyrolyzed before the PZT thin film stacking. The PZT thin films were deposited on the PT/Pt/Ti/SiO_2/Si substrate by spin-coating at 4000 rpm for 30 s. Then the PZT films were preheated at 150 °C for 5 min, pyrolyzed at 350 °C for 5 min and crystallized at 600 °C for 10 min. The PZT films were deposited for 10 cycles to obtain a thickness of 0.68 μm. Finally, another PT buffer layer was deposited and pyrolyzed on the PZT films.

X-ray diffraction (XRD) technique was used to measure structures and the crystallinity of the deposited films. Atomic force microscope (AFM) and scanning electric microscope (SEM) were used to characterize the surface morphology of the thin films and the structures of the microcantilevers.

2.2. Fabrication of microcantilevers with PT/PZT/PT thin films

The fabrication procedure of the microforce sensors with the PT/PZT/PT thin films is shown in figure 2. A 1.5 in. diameter (100) n-type, double-side-polished silicon wafer (thickness of 220 μm) was used as substrate. A 0.9 μm silicon dioxide was grown on both sides of the wafer to serve as a mask layer for back-side silicon etching. The back-side silicon dioxide layer was patterned by wet etching to define the windows of silicon cavities. The front-side silicon dioxide layer was patterned to make front-side windows that would be used to free the microcantilevers. A Pt/Ti (150 nm/50 nm) bottom electrode was deposited by RF magnetron sputtering system and wet etched using aqua-regia. The PT/PZT/PT thin films were deposited by sol–gel process. The Pt/Ti (150 nm/50 nm) top electrode was deposited and patterned by the lift-off technology. The baked PZT thin films (total thickness of 260 nm) without post-annealing were deposited

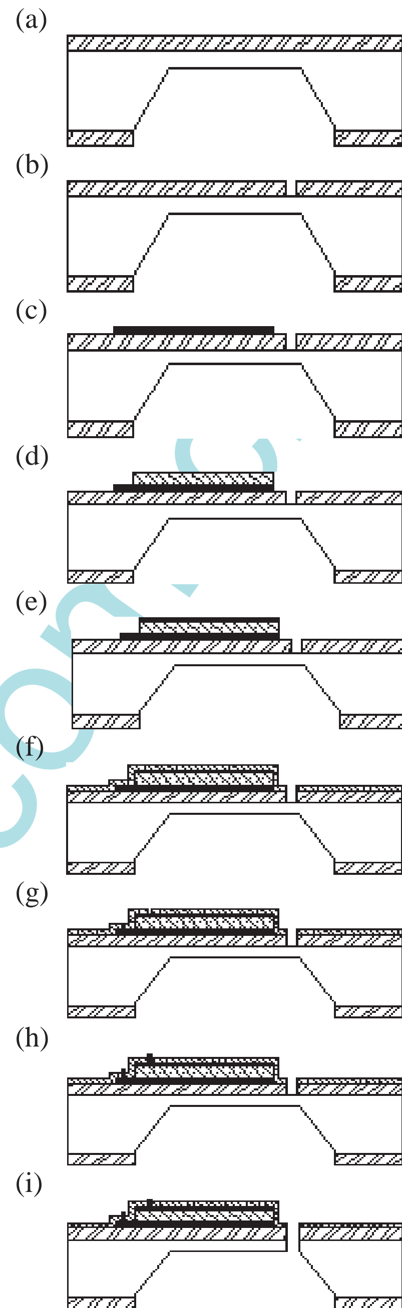

Figure 2. (a) Wet etching of bulk-Si, (b) etching of 'U' shape windows, (c) sputtering of Ti/Pt bottom electrodes, (d) deposition of the PT/PZT/PT thin films, (e) sputtering of Ti/Pt top electrodes, (f) deposition of baked PZT films for electrical isolation, (g) etching of contact holes, (h) deposition of Al bonding pads and (i) ICP of Si to free the microcantilever.

for electrical isolation. The PT/PZT/PT thin films were patterned to make contact holes and front-side windows using HF : HCl : DIH_2O (1 : 30 : 70) for about 2 min. An Al layer (thickness of 340 nm) was deposited by sputtering process and patterned using the lift-off process to form the bonding pads. An ICP process was used to dry etch the back-side silicon to define the thickness of the microcantilevers and the front-side windows to free the microcantilevers.

The SEM (JSM-6360LV, JEOL, Japan) micrograph of the microcantilevers A and B is shown in figure 3. Size A is 1000 μm in length and 200 μm in width, size B is 500 μm in length and 100 μm in width.

www.spm.com.cn

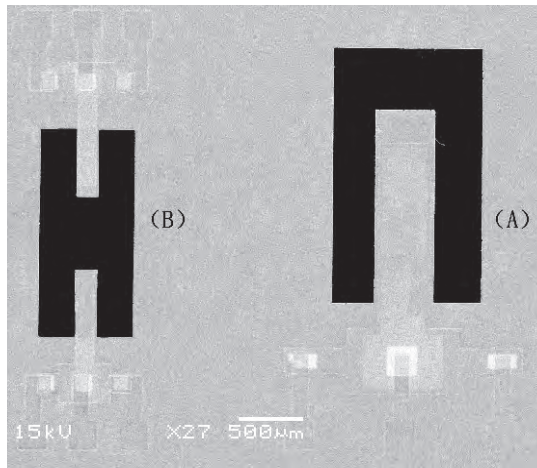

Figure 3. SEM micrograph of the microcantilevers A and B.

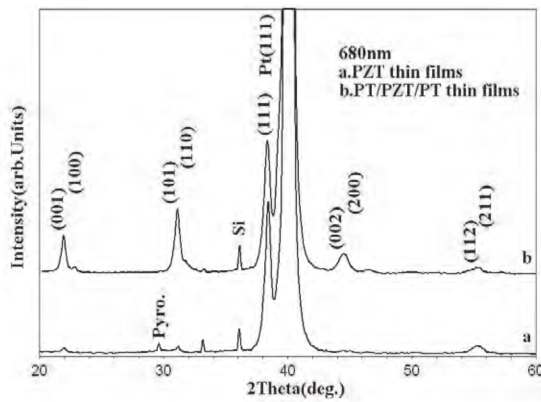

Figure 4. XRD pattern of the PZT thin films and the PT/PZT/PT thin films.

3. Results and discussion

3.1. Characterization of thin films

The XRD (XRD-6000, Shimadzu, Japan) pattern of the PZT and the PT/PZT/PT thin films is shown in figure 4, which were prepared by the one-coating-layer-annealed method [12]. The pyrochlore phase has been found in the PZT thin films, but the pure perovskite phase has been found in PT/PZT/PT thin films under the same annealing temperature. Namely, the phase formation in the PZT films is influenced by the PT buffer layer which significantly enhanced the perovskite formation. The AFM (CSPM4000) images of the PZT thin films and the PT/PZT/PT thin films are shown in figure 5. The PZT thin films and the PT/PZT/PT thin films have the grain size of 11.59 and 20.01 nm, respectively. The roughness (S_a) of the thin films is 0.99 and 6.9 nm, respectively. The AFM analysis results show that PT/PZT/PT thin films are quite smooth and dense.

3.2. Measurement of sensing properties of the microforce sensors

The measurement set-up included the driving system and the testing system. The driving system was combined with a XYZ micropositioner (TSMW13-XYZ-1A(L)), a bimorph probe and a frequency synthesizer (HPV-1C0150A0300D).

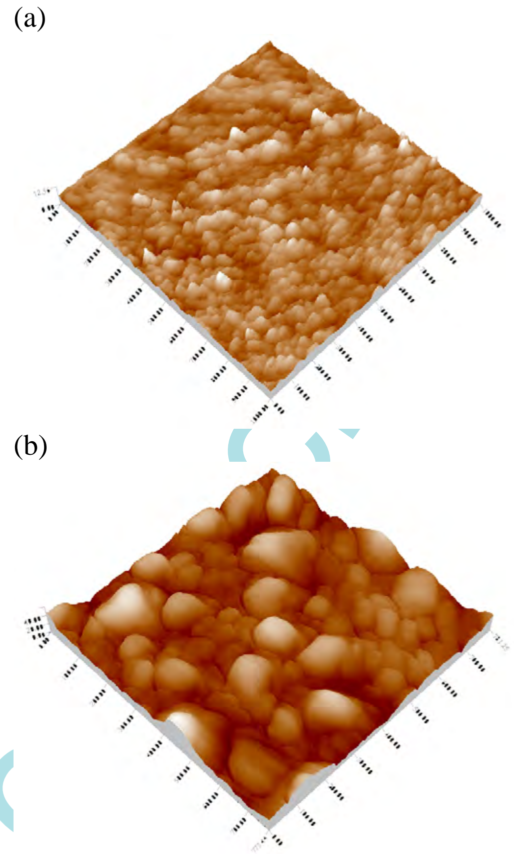

Figure 5. AFM surface morphology: (a) PZT thin films and (b) PT/PZT/PT thin films.

An electronic balance (AG245, Germany) served as the testing equipment in static state. A charge amplifier (YE5850) and a lock-in amplifier (SR830, USA) served as the testing equipment in quasi-static state. In order to minimize the error caused by the temperature and vibration, whole experiments were made on the vibration damping table in the clean room.

The bimorph probe was calibrated before the experiments, the relationship between the displacement of bimorph probe and applied dc voltage was $0.522\,\mu\mathrm{m\,V^{-1}}$. One end of the bimorph probe was fixed to the XYZ micropositioner, when the bimorph probe was statically driven by a dc voltage (resolution of 5 mV), an actuation force from the bimorph probe was loaded on the free end of the microforce sensors. The probing force was determined by the electronic balance (resolution of $0.1\,\mu$N), the spring constant of the microforce sensors was calculated by Hooke's law as

$$F = k \cdot d, \tag{1}$$

where F is the force; d is the displacement; k is the spring constant. For the experimental system, the bimorph probe was considered rigid relative to the microforce sensors. The result in static state was shown in figure 6, the microforce sensors A and B obtained spring constants of 11 and $74\,\mathrm{N\,m^{-1}}$ with the deviation of 0.36 and 0.75%, respectively. As seen in figure 6, the curves show very good linear behavior in static state, which shows good sign for the measurement in quasi-static state.

www.spm.

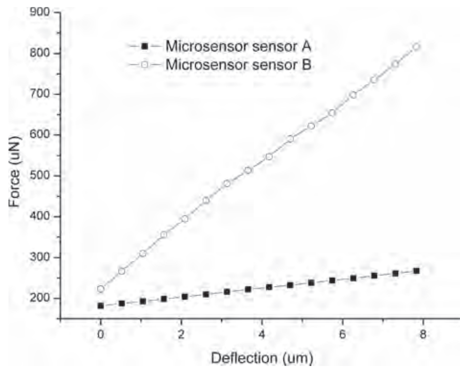

Figure 6. Spring constants of the microforce sensors A and B.

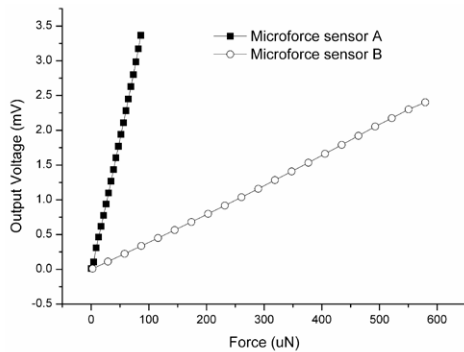

Figure 7. Sensitivities of the microforce sensors A and B.

The principle of the testing system in quasi-static state is based on Smits modes [13] as

$$Q = \frac{-3d_{31}s_{11}^{\mathrm{Si}}s_{11}^{\mathrm{P}}h_{\mathrm{Si}}(h_{\mathrm{Si}}+h_{\mathrm{P}})L^2}{K}F, \qquad (2)$$

where $K = 4s_{11}^{\mathrm{Si}}s_{11}^{\mathrm{P}}h^{\mathrm{Si}}(h^{\mathrm{P}})^3 + 4s_{11}^{\mathrm{Si}}s_{11}^{\mathrm{P}}(h^{\mathrm{Si}})^3h^{\mathrm{P}} + (s_{11}^{\mathrm{P}})^2(h^{\mathrm{Si}})^4 + (s_{11}^{\mathrm{Si}})^2(h^{\mathrm{P}})^4 + 6s_{11}^{\mathrm{Si}}s_{11}^{\mathrm{P}}(h^{\mathrm{Si}})^2(h^{\mathrm{P}})^2$, Q is the charge produced by the PZT thin film; F is the vertical force received by the PZT microcantilever free end; s_{11}^{Si} and s_{11}^{P} are the coefficients of flexibility of Si and the PZT thin film, respectively; h_{Si} and h_{P} are the thickness of Si and the PZT thin film respectively; L is the length of the PZT thin film; d_{31} is the piezoelectric coefficient of the PZT thin film. The SiO_2 layer and the electrode layer are much thinner than silicon substrate so that they are ignored. Though the PT/PZT/PT thin films are also thin, they are used as piezoelectric layer which can produce the charge.

The charge measurements (80 Hz) were made with the charge amplifier, and gained with the lock-in amplifier. The result was shown in figure 7, the PT/PZT/PT microforce sensors A and B obtained the sensitivities of 0.040 and 0.004 mVμN^{-1} with resolution of 28 and 19 μN, respectively, both microforce sensors obtained very good linearity behavior. The sensitivity of microforce sensor A is higher than the microforce sensor B, but the resolution is in opposite way.

4. Conclusions

The PT/PZT/PT thin films were fabricated by the sol–gel process. The PT buffer layer is required to effectively enhance the perovskite formation of the PZT films. Good linearity of force and deflection curves were obtained in static state, good linearity of microforce response was obtained in quasi-static state as well as for the microforce sensors. Combined with the micromachining processes, the PT/PZT/PT thin films were shown to be good candidate materials for developing the application of microforce sensors.

Acknowledgments

This work was supported by the National Natural Science Foundation of China (nos 90207003 and 90607002).

References

[1] Takayama R and Tomita Y 1989 *J. Appl. Phys.* **65** 1666
[2] Muralt P, Kohli M, Maeder T, Kholkin A, Brooks K, Setter N and Luthier R 1995 *Sensors Actuators* A **48** 157
[3] Lee C, Itoh T and Suga T 1999 *Sensors Actuators* A **72** 179–88
[4] DeVoe D L and Pisano A P 2001 *J. Microelectromech. Syst.* **10** 180
[5] Wang L-P, Wolf J, Wang Y, Deng K K, Zou L, Davis R J and Susan T-M 2003 *J. Microelectromech. Syst.* **12** 433
[6] Luginbuhl P, Racine G A, Lerch P, Romanowicz B, Brooks K G, de Rooij N F, Renaud P and Setter N 1996 *Sensors Actuators* A **54** 530
[7] Kueppers H, Leuerer T, Schnakenberg U and Mokwa W 2002 *Sensors Actuators* A **97/98** 680
[8] Scott J F, Parris M, Traynor S, Ottenbacher V, Shawabkeh A and Oliver W F 1988 *J. Appl. Phys.* **64** 787
[9] Kwok C K and Desu S B 1993 *J. Mater. Res.* **8** 339
[10] Ren T-L, Zhang L-T, Lin L-T and Li Z-J 2001 *Chin. Phys. Lett.* **18** 132
[11] Doi H, Atsuki T, Soyama N, Sasaki G, Yonezawa T and Ogi K 1994 *Japan. J. Appl. Phys.* **33** 5159
[12] Liu M, Wang J, Wang L and Cui T 2007 *Smart. Mater. Struct.* **16** 93
[13] Smits J G and Choi W-S 1991 IEEE *Trans. Ultrason, Ferro., Freq. Control* **38** 256

www.spm.com.cn